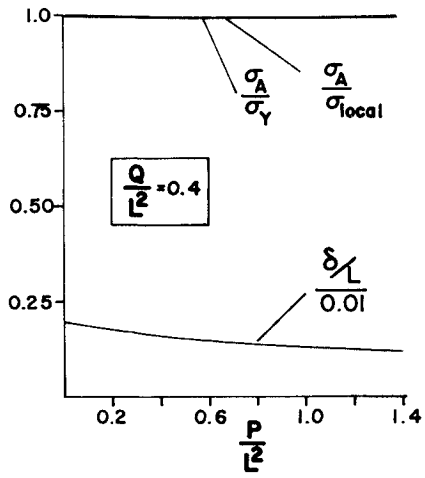

Fig. 4 Activity of constraints for mild steel beam column.

under suppression of local buckling and yielding the optimum mild steel tube has active local and yield constraints with inherent stiffness considerably in excess of a 1% deflection limitation. The discontinuous behavior of t/L and D/L where $P/L^2 < 0.35$ for the case $Q/L^2 = 0$ in Fig. 3 accompanied by continuity in weight merit (Fig. 2) shows the existence of multiple optima for the simple column beyond the load index for which the yield constraint becomes active. The corresponding inactivity of either the local or Euler modes or a combination gives rise to a family of cross sections each having the property of least weight. Although no unique pair (t, D) can be found from the programed solution, their product is computable so as to achieve the yielding area, and then either the local or Euler constraints can be set equal to yield stress to effect a unique sizing.

References

[1] Michell, A. G. M., "The Limits of Economy of Material in Frame-Structures," *Philosophical Magazine*, Vol. 8, 1904, pp. 589–597.

[2] Wagner, H., "Remarks on Airplane Struts and Girders Under Compressive and Bending Stresses. Index Values," TM 500, 1929, NACA.

[3] Farrar, D. J., "The Design of Compression Structures for Minimum Weight," *Journal of the Royal Aeronautical Society*, Vol. 53, 1949, pp. 1041–1052.

[4] Shanley, F. R., "Principles of Structural Design for Minimum Weight," *Journal of Aeronautical Science*, Vol. 16, No. 3, 1949.

[5] Gerard, G., *Minimum Weight Analysis of Compression Structures*, New York University Press, New York, 1952.

[6] Cox, H. L., *The Design of Structures of Least Weight*, Pergamon Press, London, 1965.

[7] Wasiutynski, Z. and Brandt, A., "The Present State of Knowledge in the Field of Optimum Design of Structures," *Applied Mechanics Reviews*, Vol. 16, No. 5, 1953.

[8] Sheu, C. Y. and Prager, W., "Recent Developments in Optimal Structural Design," *Applied Mechanics Reviews*, Vol. 21, No. 10, 1968.

[9] Pope, G. G. and Schmit, L. A., "Structural Design Applications of Mathematical Programming Techniques," AGARDograph 149, 1971.

[10] Spunt, L., *Optimum Structural Design*, Prentice-Hall, Englewood Cliffs, N.J., 1971.

[11] Krzyś, W. and Życzkowski, M., "A Certain Method of Parametrical Structural Optimum Shape-design," *Bulletin De L'academie*, Vol. XI, No. 10, 1963.

[12] Spunt, L., "Weight Optimization of the Postbuckled Integrally Stiffened Wide Column," *Journal of Aircraft*, Vol. 7, No. 4, July-Aug. 1970, pp. 330–333.

[13] Schmit, L. A., Kichner, T. P., and Morrow, W. M., "Structural Synthesis Capability for Integrally Stiffened Waffle Plates," *AIAA Journal*, Vol. 1, No. 12, Dec. 1963, pp. 2820–2836.

[14] Dorn, W. S., Gomory, R. E., and Greenberg, H. H., "Automatic Design of Optimal Structures," *Journal de Mécanique*, Vol. 3, No. 1, 1964.

[15] Wilde, D. J. and Beightler, C. S., *Foundations of Optimization*, Prentice-Hall, Englewood Cliffs, N.J., 1967.

[16] Burns, A. B. and Skogh, J., "Combined Loads Minimum Weight Analysis of Stiffened Plates and Shells," *Journal of Spacecraft*, Vol. 3, No. 2, Feb. 1966, pp. 235–240.

[17] Switzky, H., "The Minimum Weight Design of Structures Operating in an Aerospace Environment," ASD-TDR-62-763, 1962, Wright-Patterson Air Force Base, Ohio.

[18] Felton, L. P. and Dobbs, M. W., "Optimum Design of Tubes for Bending and Torsion," *Proceedings of the ASCE*, Vol. 92, ST 4, Aug. 1967.

[19] Timoshenko, S. P. and Gere, J. M., *Theory of Elastic Stability*, McGraw-Hill, New York, 1961.

Floating Piecewise Linear Approximation of a Nonlinear Constitutive Equation

DAVID DURBAN* AND MENAHEM BARUCH†
Technion—Israel Institute of Technology, Haifa, Israel

Introduction

ONE of the main difficulties arising in large deflection analysis of structures has its origin in the nonlinearity of the stress-strain relations. This difficulty is usually overcome by piecewise linearization of the constitutive equation. A method for construction of the "best" piecewise linear approximation is proposed. It will be shown, through an examination of a simple model, that the suggested method yields a sequence of upper bounds to the load-deflection behavior. The maximum load carrying capacities for the given model obtained by the approximate and the exact methods are the same.

Exact Solution to a Simple Model

Consider the simple model shown in Fig. 1. This model is taken from Ref. 1 where an approximate analysis has been given. The model consists of a rigid bar AB and a spring BC. The stress strain relation of the spring is given by

$$\theta - \theta_o = (\sigma/E) + K(\sigma/E)^n \tag{1}$$

where σ is the stress in the spring and θ_o is an initial imperfection. Equation (1) is of the type given in Ref. 2. The static equilibrium requirement, for small value of θ ($tg\theta \approx \theta$) is

$$A\sigma = P\theta \tag{2}$$

where A is the area of the spring and P the external applied load. By substitution of Eq. (2) into Eq. (1), the exact load-deflection behavior is obtained

$$\theta - \theta_o = (P\theta/EA) + K(P\theta/EA)^n \tag{3}$$

The behavior of the perfect system is obtained from Eq. (3) by taking $\theta_o = 0$. The resulting nonlinear equation has two branches

$$\theta = 0 \quad \text{and} \quad (P/EA)[1 + K(P\theta/EA)^{n-1}] = 1 \tag{4}$$

Received May 29, 1973. This work is based on a part of a thesis to be submitted to the Technion—Israel Institute of Technology, Haifa, in partial fulfilment of the requirements for the Degree of Doctor of Science. The research reported in this Note has been sponsored in part by the Air Force Office of Scientific Research, U.S. Air Force, under Grant 72-2394. The authors would like to thank E. Shaish of the Department of Aeronautical Engineering, Technion, for his assistance in the computational work.

Index category: Structural Stability Analysis.

* Instructor, Department of Aeronautical Engineering.

† Associate Professor, Department of Aeronautical Engineering. Member AIAA.

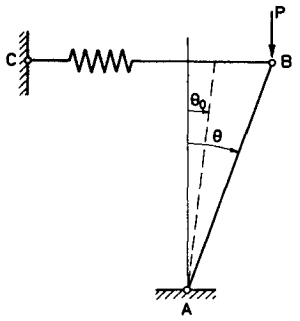

Fig. 1 A simple model.

with the bifurcation point

$$\theta_{cr} = 0 \qquad P_{cr}/EA = 1 \tag{5}$$

The imperfect system Eq. (3) has no branching point and its instability is obtained at the maximum possible load P^* (at which $dP/d\theta = 0$). Differentiating Eq. (3) yields

$$1 = \frac{P^*}{P_{cr}}\left[1 + nK\left(\frac{P^*}{P_{cr}}\theta^*\right)^{n-1}\right] \tag{6}$$

and also

$$\theta^* - \theta_o = \frac{P^*}{P_{cr}}\theta^* + K\left(\frac{P^*}{P_{cr}}\theta^*\right)^n \tag{7}$$

where θ^* is the angle corresponding to P^*. Fortunately Eqs. (6) and (7) admit a simple solution

$$\frac{P^*}{P_{cr}} = 1\Big/\left[1 + nK^{1/n}\left(\frac{\theta_o}{n-1}\right)^{(n-1)/n}\right] \tag{8}$$

$$\theta^* = \frac{n\theta_o}{n-1} + \left[\frac{\theta_o}{(n-1)K}\right]^{1/n} \tag{9}$$

Typical results for the perfect and the imperfect system are shown in Figs. 2 and 3.

The Lowest Modulus Concept

Before proceeding, the concept of the lowest modulus will be introduced. This modulus will be used later in the approximate analysis of the model.

Consider again the Ramberg Osgood stress strain relation

$$\varepsilon = (\sigma/E) + K(\sigma/E)^n \tag{10}$$

and suppose that Eq. (10) is replaced by the two tangents OA and ABC (Fig. 4). The slope of the first tangent is the regular

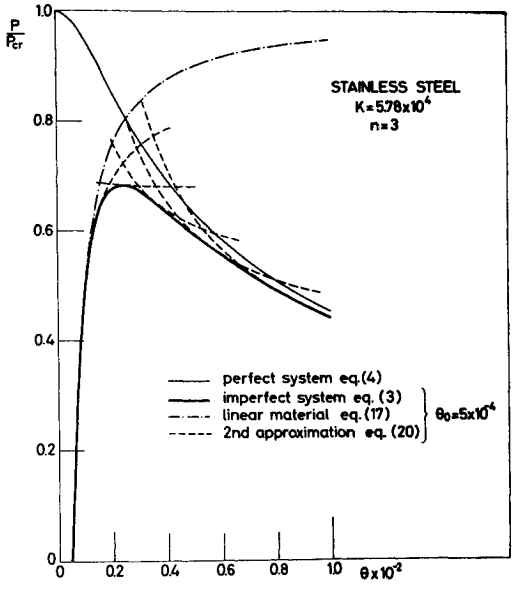

Fig. 2 Load deflection behavior, stainless steel.

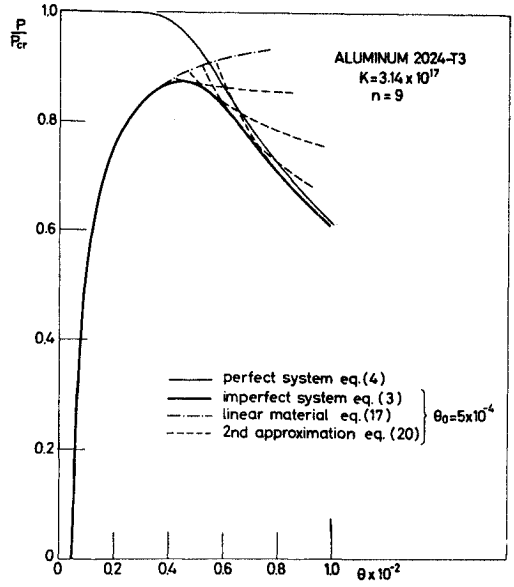

Fig. 3 Load deflection behavior, 2024-T3 Aluminum.

modulus of elasticity E. Let the slope of the second tangent be E_L. It is understood, at least intuitively, that the two tangents represent a stiffer material than the one given by Eq. (10). It appears also that E_L is the lowest possible modulus for a straight line starting at A and assuring a stiffer material than Eq. (10).

The lowest modulus can be expressed in terms of ε_1, σ_1; the involved quantities have to satisfy the following relations

$$\varepsilon_1 = \sigma_1/E \tag{11a}$$

$$\varepsilon_2 = (\sigma_2/E) + K(\sigma_2/E)^n \tag{11b}$$

$$E_L = E/[1 + nK(\sigma_2/E)^{n-1}] \tag{11c}$$

$$E_L = (\sigma_2 - \sigma_1)/(\varepsilon_2 - \varepsilon_1) \tag{11d}$$

and the desired solution of Eqs. (11a–d) is obtained, after some algebraic manipulations, as

$$E_L = \frac{E}{1 + NnK(\sigma_1/E)^{n-1}} \tag{12}$$

where

$$N = [n/(n-1)]^{n-1} \tag{13}$$

The lowest modulus E_L is, of course, smaller than the "tangent modulus" at the stress level σ_1

$$E_t = \frac{E}{1 + nK(\sigma_1/E)^{n-1}} \tag{14}$$

and obviously $E_L < E_t$. Note also that for ideal elasto-plastic case ($n \to \infty$) an interesting limit exists

$$\lim_{n\to\infty} N = e \tag{15}$$

Approximate Solution of the Model

Returning to the model of Fig. 1, the exact stress strain relation Eq. (1) is replaced by the two tangents shown in Fig. 4. The analysis is now carried separately for each line.

In segment OA

$$\sigma/E = \theta - \theta_o \qquad \theta_o \leqq \theta \leqq \theta_1 \tag{16}$$

and substituting from Eq. (2)

$$P/P_{cr} = 1 - (\theta_o/\theta) \qquad \theta_o \leqq \theta \leqq \theta_1 \tag{17}$$

Equation (17) describes the load deflection behavior for a linear material.

In segment AC

$$\sigma = E(\theta_1 - \theta_o) + E_L(\theta - \theta_1) \qquad \theta \geqq \theta_1 \tag{18}$$

but from Eqs. (12) and (16)

$$E_L = \frac{E}{1 + NnK(\theta_1 - \theta_o)^{n-1}} \tag{19}$$

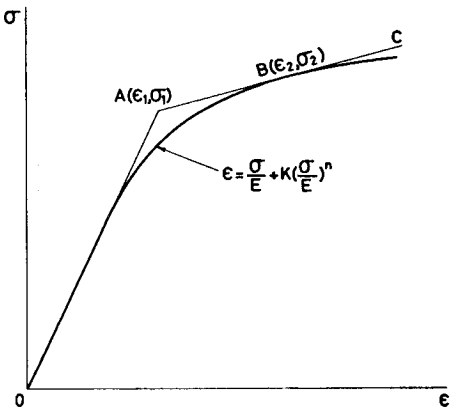

Fig. 4 The lowest modulus.

Combining Eqs. (2, 18, and 19) yields finally

$$\frac{P}{P_{cr}} = \frac{\theta_1 - \theta_o}{\theta} + \frac{1-(\theta_1/\theta)}{1+NnK(\theta_1-\theta_o)^{n-1}} \qquad \theta \geqq \theta_1 \tag{20}$$

Equations (17) and (20) describe the behavior of a material which is stiffer than the true material. Hence the curve P/P_{cr} vs θ obtained from these equations is an upper bound for the real curve.

Regarding θ_1 (point A in Fig. 4) as a floating parameter and changing it in small steps, a sequence of curves is obtained. Numerical results for two materials are shown in Figs. 2 and 3. Also, the exact results obtained before are shown.

The envelope formed by the family of the curves given by Eq. (20) can be found in the usual way. Equation (20) is rewritten in the form

$$F(P,\theta,\theta_1) = (P/P_{cr})[1+NnK(\theta_1-\theta_o)^{n-1}]\theta - NnK(\theta_1-\theta_o)^n - \theta + \theta_o = 0 \tag{21}$$

The envelope is obtained[3] by considering, simultaneously, Eq. (21) and the equation

$$\frac{\partial F}{\partial \theta_1} = \frac{P}{P_{cr}} Nn(n-1)K(\theta_1-\theta_o)^{n-2}\theta - Nn^2K(\theta_1-\theta_o)^{n-1} = 0 \tag{22}$$

or

$$\theta_1 - \theta_o = [(n-1)/n](P/P_{cr})\theta \tag{23}$$

Substitution of Eq. (23) into Eq. (21) yields the exact solution, Eq. (3). Thus, the envelope of the approximate solutions, Eq. (20), is the true behavior of the model.

The maximum load carrying capacity (for the given model) of the approximated system can be obtained as follows: differentiating Eq. (20) yields

$$\frac{d}{d\theta}\left(\frac{P}{P_{cr}}\right) = \frac{1}{\theta^2} \cdot \frac{\theta_o - NnK(\theta_1-\theta_o)^n}{1+NnK(\theta_1-\theta_o)^{n-1}} \tag{24}$$

Thus, the load increment in the second segment given by Eq. (20) is positive or negative according to the sign of the numerator in Eq. (24). Equating Eq. (24) to zero, the point $\theta_1 = \theta_1{}^{**}$, where there is no load increment from Eq. (20), is obtained

$$\theta_o - NnK(\theta_1{}^{**} - \theta_o)^n = 0 \tag{25}$$

The solution of Eq. (25) is

$$\theta_1{}^{**} = \theta_o + [(n-1)/n][\theta_o/(n-1)K]^{1/n} \tag{26}$$

and note that [see Eq. (9)]

$$\theta_1{}^{**} = [(n-1)/n]\theta^* \tag{27}$$

The maximum load for the approximate system, P^{**}, is obtained by substituting Eq. (26) into Eq. (20)

$$\frac{P^{**}}{P_{cr}} = 1 \Big/ \left[1 + nK^{1/n}\left(\frac{\theta_o}{n-1}\right)^{(n-1)/n}\right] \tag{28}$$

which is, of course, the same as the exact solution Eq. (8).

Finally it should be pointed out that the "lowest modulus" $E_L{}^{**}$ corresponding to P^{**}, is equal to the tangent modulus $E_t{}^*$ which corresponds to P^*, and that the following relations hold

$$E_t{}^*/E = P^*/P_{cr} = P^{**}/P_{cr} = E_L{}^{**}/E \tag{29}$$

Conclusions

It has been shown that, for the simple model considered, the envelope of the floating piecewise linear approximation represents the exact nonlinear solution.

References

[1] Drucker, D. C. and Onat, E. T., "On the Concept of Stability of Inelastic Systems," *Journal of the Aerospace Sciences*, Vol. 21, 1954, pp. 543–548, 565.

[2] Ramberg, W. and Osgood, W. R., "Description of Stress-Strain Curves by Three Parameters," TN 902, 1943, NACA.

[3] Courant, R., *Differential and Integral Calculus*, Vol. II, Blackie and Son Ltd., London, 1936, pp. 171–179.

Measurements in the Near Field of Supersonic Nozzles for Chemical Laser Systems

D. L. WHITFIELD,* J. W. L. LEWIS,†

AND

W. D. WILLIAMS‡

ARO Inc., Arnold Air Force Station, Tenn.

Introduction

As a contribution to the design of laser systems involving banks of multiple nozzles, the flowfields and gas mixing characteristics near the exits of two Direct Combustion Laser (DCL) nozzle banks were investigated using simulated exhaust gases.[1] The experimental techniques used in the investigation were: 1) laser Doppler velocimeter to measure flow velocities, 2) probes to measure pitot pressure, 3) electron beam to measure both relative and absolute specie number densities, and 4) electron beam to make flow visualization photographs. Also, an analytical investigation was conducted of the flow inside the nozzles, and these results were in good agreement with the experimental data.[1] Only selected results for one nozzle bank are presented in this Note.

DCL Nozzle Banks

The DCL nozzle banks were supplied by the Air Force Rocket Propulsion Lab. The nozzle bank corresponding to the present data was made of nickel. It had conical nozzles with exit diameters (d_e) of 0.234 in., area ratios of 16.85, 10° divergent wall half angles, and 0.024-in.-diam H_2 orifices. A schematic is given in Fig. 1 of the locations of four profiles for which measurements

Received July 12, 1973; presented as Paper 73-642 at the AIAA 6th Fluid and Plasma Dynamics Conference, Palm Springs, Calif., July 16–18, 1973; revision received December 26, 1973. This work was sponsored by the Air Force Rocket Propulsion Laboratory (AFRPL), Air Force Systems Command (AFSC), and the Air Force Weapons Laboratory (AFWL), AFSC. The results were obtained by ARO Inc., contract operator of the Arnold Engineering Development Center (AEDC), AFSC, Arnold Air Force Station, Tenn.

Index categories: Jets, Wakes, and Viscid-Inviscid Flow Interactions; Nozzle and Channel Flow; Lasers.

* Research Engineer, 16-P Section, Propulsion Wind-Tunnel Facility. Member AIAA.

† Senior Scientist, Aerospace Projects Branch, von Kármán Gas Dynamics Facility.

‡ Research Engineer, Aerospace Projects Branch, von Kármán Gas Dynamics Facility.